Towards diamond micro four-point probes

Han, Anpan; Hartmann Henrichsen, Henrik; Savenko, Aleksei ; Petersen, Dirch Hjorth; Hansen, Ole

Published in:
Micro and Nano Engineering

Link to article, DOI:
10.1016/j.mne.2019.05.002

Publication date:
2019

Document Version
Publisher's PDF, also known as Version of record

Micro and Nano Engineering 5 (2019) 100037

Contents lists available at ScienceDirect

Micro and Nano Engineering

journal homepage: www.journals.elsevier.com/micro-and-nano-engineering

Research paper

Towards diamond micro four-point probes

Anpan Han[a,*], Henrik Hartmann Henrichsen[b], Aleksei Savenko[c,1], Dirch Hjorth Petersen[c], Ole Hansen[d]

[a] Department of Mechanical Engineering, Technical University of Denmark (DTU), Produktionstorvet, Building 425, Kgs. Lyngby 2800, Denmark
[b] CAPRES – a KLA company, Diplomvej, Building 373, 2800 Kgs. Lyngby, Denmark
[c] Department of Physics, DTU, Fysikvej, Building 307, 2800 Kgs. Lyngby, Denmark
[d] DTU Nanolab, DTU, Oersteds Plads, Building 347, 2800 Kgs. Lyngby, Denmark

ARTICLE INFO

Keywords:
Diamond MEMS
Diamond cantilevers
Micro four-point probes
Polycrystalline diamond thin-film

ABSTRACT

Diamond has extreme physical properties, and it is used for critical applications in micro- and nanotechnology and nanosciences. Micro four-point probes for electrical characterization of metal and semiconductor thin-films are made from metal coated silicon microcantilevers. The limiting factors in probe lifetime are frictional wear and thermal damage from electrical overstress. Diamond has superior thermal conductivity and wear resistant properties which could improve probe lifetime. In this paper, we present wafer-level fabrication of polycrystalline diamond micro cantilevers for micro four-point probe applications. The process only requires two photolithography steps. We show great design flexibility and demonstrate extremely mechanical robust free-standing diamond cantilever up to 300 μm long. We believe that this process may find important applications beyond micro four-point probes. The next step is to implement micro four-point probes using high quality electrically conductive diamond when it becomes available.

1. Introduction

Diamond is fantastic material with exceptional physical properties (Table 1). For example, it is the hardest material, and it has the highest thermal conductivity. Because of its superior properties, micro- and nanostructures in diamond have unrivaled characteristics compared to silicon. The Young's modulus of diamond is 1200 GPa, which is 10 times higher than that of silicon. Diamond is also 10 times harder and 5 times stronger (tensile strength) than silicon. There are two classes of diamond substrates readily available for micro and nanotechnology; single crystalline diamond (SCD) which is expensive, and the size is limited to $3 \times 3 \times 0.5$ mm, and poly crystalline thin-film diamond (PCD) which is grown by e.g. hot filament CVD onto wafer sized silicon substrates. PCD can be grown on silicon wafers coated with silicon dioxide, and the product is called diamond on oxide (DOI) which can be processed similar to silicon on insulator (SOI) wafers. The thickness of the buried oxide layer (BOX) is typically 1 μm. The thickness of the PVD is between 100 and 2000 nm. The grain size can be engineered to between 3 nm [1] and 1 μm. The surface roughness of thin-films with 3 nm grain size is only a few nanometers [1], while the surface is more rough for larger grain size. The thermal conductivity of PCD is highly dependent on the grain size and film thickness because of phonon scattering at the grain boundaries. While the thermal conductivity of bulk *gem* diamond is 2300 W/(m K), due to phonon scattering at grain boundaries, PCD values range between 12 and 2200 W/(mK) [2,3]. The electrical properties of PCD can be tuned by hole doping (p-type) with boron or electron doping with nitrogen (n-type). Conductive PCD with resistivity as low as 0.005 Ωcm [4] can be obtained. PCD offers a powerful material and technology platform for MEMS and NEMS [5]. Examples are biosensors [6], coatings for implantable medical MEMS [7], and high frequency NEMS resonators [8].

We are especially interested in micro four-point probes (M4PP) for accurate measurement of thin-film sheet resistance on materials such as graphene [16], ultra-shallow semiconductors junctions [17,18] and magnetic tunnel junctions [19,20]. The state-of-the-art micro-fabricated M4PP has four micro cantilevers made from polycrystalline silicon that are coated with 200 nm of nickel thin-film [21]. The M4PP probe is mounted with the nickel thin-film facing down, and the angle between the probe cantilevers and the sample is 45°. The nickel thin-film makes physical contact with the sample and carries the electrical current required for characterization. The body of the probe is very similar to that of the atomic force microscope (AFM) probe. The state-

* Corresponding author.
E-mail address: anph@mek.dtu.dk (A. Han).
[1] Now at Thermofisher (FEI), 5651 GG Eindhoven, The Netherlands.

https://doi.org/10.1016/j.mne.2019.05.002
Received 5 March 2018; Received in revised form 12 April 2019; Accepted 3 May 2019

Table 1
Material properties of CVD diamond compared to silicon and silicon carbide.

Material	Young's modulus (GPa)	Fracture strength (GPa)	Fracture toughness (MPa $m^{½}$)	Friction coeff.	Ref.
Silicon	150	0.3	1.6	0.2–0.7	[9,10]
SiC	373	1.44	4	0.2–0.5	[11,12]
UNCD	400–1100	1–5	4–9	0.008–0.05	[13] [14]
MCD (this study)	800–1200	1–5	5–9	0.1	[13,15]

of-the-art technology can be improved in several areas. Most importantly, we must improve the life time of the probes. Because of the slight sliding motion every time the nickel coated cantilever makes physical contact with the sample, the nickel film wears out, and the M4PP must be changed and discarded. One way to reduce frictional wear is to make "three-way" flexible electrodes [22,23]. Another approach could be to use diamond. Because diamond is extremely hard, and it has a low friction coefficient (Table 1), it has outstanding wear and tribology properties [24,25]. Diamond coatings are used for most demanding anti-wear applications. If the entire cantilever can be made from conductive diamond, it would be virtually impossible to wear out such probes. Furthermore, AFM using conductive diamond coated probes are regularly used for electrical characterization of semiconductors [26]. Based on the above facts, it became obvious that conductive diamond M4PP could prove a useful alternative to polycrystalline silicon cantilevers. In this paper, we present microfabricated polycrystalline diamond cantilevers for M4PP applications.

2. Materials and methods

2.1. Polycrystalline diamond M4PP fabrication process

The starting substrates are AQUA50 DOI wafers from Advanced Diamond Technologies, USA (Fig. 1a). To be compatible with the measurement instrument that is designed for silicon 4PP, we needed diamond 4PPs that have approximate the same length and spring constant as the silicon 4PP. This is achieved by selecting a thinner diamond film, which is nominally 1-μm-thick (silicon probes are 7-μm-thick). The buried oxide layer (BOX) is 1-μm-thick, the substrate is a 500-μm-thick silicon wafer 100 mm in diameter. The DOI wafers have silicon dioxide layers on both sides and a very thin layer of PCD on the back side of the wafer. These thin-films on the backside were removed (Fig. 1b). We removed the backside PCD by inductively coupled plasma (ICP) etching using a MESC Multiplex ICP instrument from STPS, UK. The process parameters were 30 sccm Ar, 90 sccm O_2, 1000 W coil power, 200 W platen power, and 20 mTorr pressure. This process is referred as the "diamond etch". To remove the backside silicon dioxide the wafer was wet etched in buffered HF. We used photolithography and lift-off to pattern Al, which is used as etch-mask for both diamond and deep reactive ion etching (DRIE) of silicon (Fig. 1c). The thickness of Al mask was 200 nm. We optimized a DRIE process to etch silicon from the backside (Fig. 1d). Diamond etch was used to etch the diamond thin-film (Fig. 1e). The remaining Al mask was removed in AZ 400 K photoresist developer that contains KOH (Fig. 1f), and buffered HF was used for release diamond cantilevers from the DOI substrate (Fig. 1g). To reduce the series resistance of the probes and the electrical leads to the bonding pad, a metal layer was evaporated on top of the diamond after the BHF release (Fig. 1 h1). This process step is well established for the fabrication of commercial M4PP, which utilize the undercut in the oxide BOX layer to avoid electrical short circuit (Fig. 1 h2) [27].

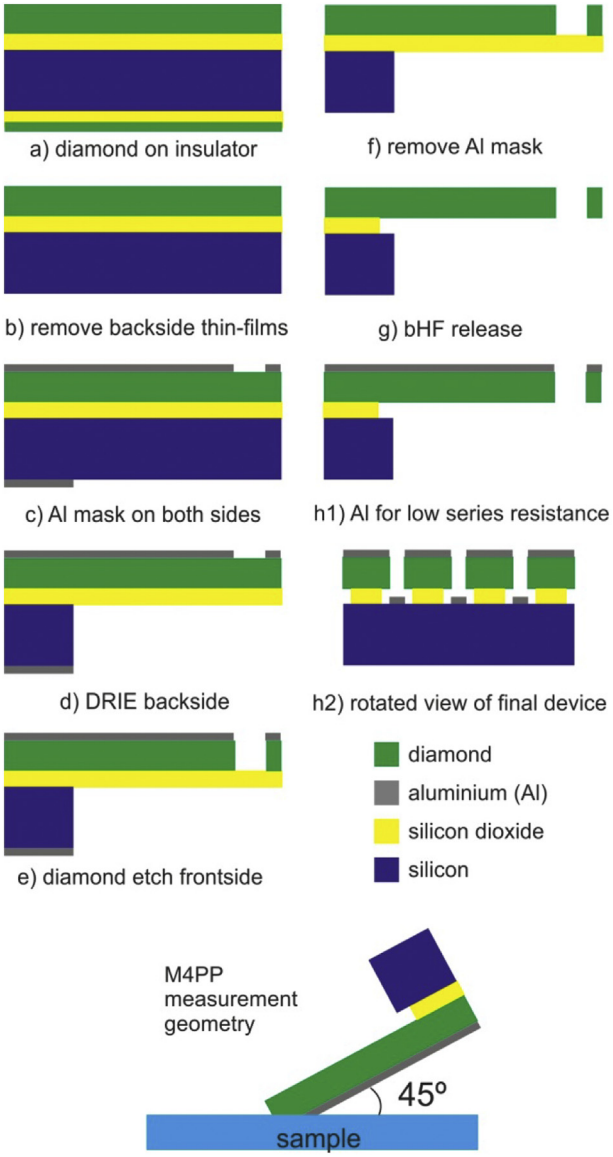

Fig. 1. Diamond M4PP fabrication process and M4PP measurement geometry.

3. Results and discussions

3.1. Fabrication process

When designing the fabrication process, we carefully considered three important aspects. Firstly, the advantages of diamond and added value must not be compromised by complicated MEMS processes. Secondly, we would like to have production flexibility such that we can select an optimal MEMS foundry, and hence we must design a transferable process. Thirdly, the MEMS design and process must not be a radically different such it would compromise downstream processes for MPP production and applications such as packaging and measurement. We devised an efficient MEMS compatible process that only requires two photolithography masks without compromising downstream processes by keeping the original M4PP die, probe, current leads and wire bonding designs. To release the cantilevers, we used a more efficient DRIE process instead of the original aqueous KOH based release. With the DRIE process, we avoid one silicon nitride masking layer and its removal.

As shown in Fig. 2, we successfully fabricated PCD M4PPs. A single die is 4 mm by 1.6 mm (Fig. 2a). We designed full-size wire bonding

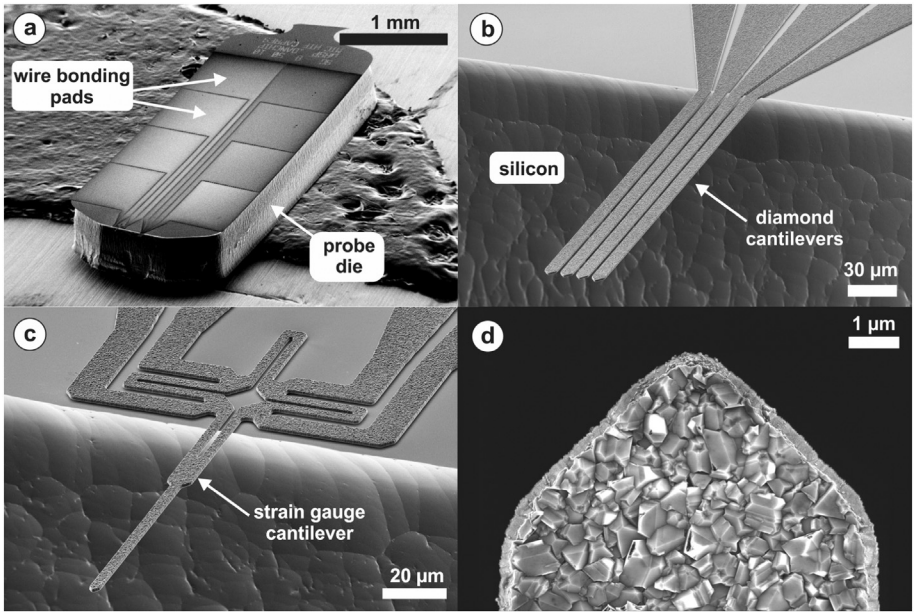

Fig. 2. Diamond M4PP with integrated strain gauge cantilever for surface detection. SEM image of M4PP (a), probe cantilevers (b), integrated strain gauge sensor and cantilever (c). The tip of the diamond cantilever at high magnification (d). Images are taken before final metallization step.

pads that are easy to access during the wire bonding process. For each M4PP probe, there are 4 diamond cantilevers protruding from the silicon probe chip (Fig. 2b). We inspected the probes from different angles by SEM, and we observed that the cantilevers protruded from the silicon probe extremely straight, which proves that we did not induce any undesired stress during fabrication. On the same M4PP probe we integrated a strain gauge cantilever sensor used for surface detection [18] (Fig. 2c). Fig. 2d shows a high magnification of the tip of a cantilever. We observed the facets of the micrometer sized diamond crystals. There is a 300 nm wide "strip" around the tip, and which is the projection of the positive etch angle that is shown later. At the edge of the cantilever, we see that the crystals are "cut" by the etching process. This observation is important because we can then make structures smaller than the grain size. For 4PP measurements, diamond probes made from diamond thin-films with very rough surface may scratch the sample. To reduce the surface roughness and also the friction coefficient (Table 1), we could either select a diamond thin-film with 3 nm grainsize [1], or use the smooth diamond surface facing the oxide layer.

The most challenging process step is diamond etching. Compared to etching silicon, there are only a few reports on diamond etching processes. We selectively list etching processes in Table 2. See also Castelletto et al. for a recent review on diamond nanofabrication [28]. There are two strategies for etching diamond. Either an O_2 and CF_4 plasma combined with a SiO_2 mask, or an O_2 and Ar plasma combined with a metal mask. The etch-rates ranged between 50 and 660 nm/min, and they are very instrument dependent. The etch selectivities of diamond over etch mask are between 8 and 50. For our application, the etching processes must be compatible with most MEMS foundries, and for high resource efficiency, we needed to etch through the PCD layer quickly. Therefore we needed high etch rate, good selectivity, and masking materials that are MEMS compatible. This is possible by using an Al hard mask combined with O_2/Ar plasma chemistry. We used a 200-nm-thick Al mask, and the etch process parameters were 30 sccm Ar, 90 sccm O_2, 1000 W coil power, 200 W platen bias, and 20 mTorr pressure. The etch rate was measured to 90 nm/min, and the etch selectivity was above 8, which is adequate for etching our PCD thin-film. However, the etch rate is lower than previous reports [29,30], which we attribute to the difference between the instruments. The etch profile was measure by SEM to 76° (Fig. 3). For our 1200-nm-thick PCD film, the bottom of the film is 300 nm wider than the top, which is tolerable for M4PP applications. For applications that strictly require vertical walls, we could optimize the etch profile by reducing the platen power [29].

Our process is a full wafer process, and we can fit 330 probes onto a single wafer. We took advantage of this design freedom, and on the very same wafer we included 14 different designs with different applications in mind. For example as shown in Fig. 4, we designed the spring constant by changing the cantilever length and width to control the contact force. And by changing the tip shape we control the contact pressure and penetration depth, as the ideal contact conditions may be different for different materials. Fig. 4c shows SEM images of cantilevers with tip angles very sharp (24°), sharp 90° or blunt. Using optical microscopy and SEM, we did not observe significant wafer level variation of the tip shape nor the distance between probe cantilevers. However, the cantilever length is slightly shorter in areas near the wafer center compared to areas towards the edge of the wafer. The variation is induced in DRIE backside process step (Fig. 1d), and it is caused by the DRIE loading effect which etch the center areas slower than the edge areas, which

Table 2
Plasma etching of diamond.

Reference	Year	Instrument	Plasma chemistry	Mask	Etch rate (nm/min)	Selectivity
Ando et al. [32]	2002	RIE	O_2/CF_4	SiO_2	150	–
Hwang et al. [29]	2004	ICP	O_2/Ar	Al	660	50
Ding et al. [30]	2005	RIE	O_2/Ar	Ni	50	–
Yamada et al. [33]	2007	ICP	O_2/CF_4	SiO_2	340	10–26
Hausmann et al. [34]	2010	ICP	O_2	Au, Al_2O_3, SiO_2	200	1:8
This work	2019	ICP	O_2/Ar	Al	90	8

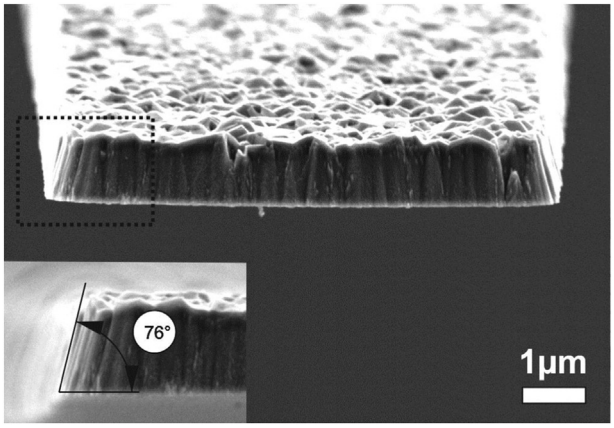

Fig. 3. SEM image of a diamond cantilever with blunt tip. Image is taken from the front with the cantilever tip slightly tilted down. The inset shows front view of the area inside the rectangle with dotted outline. The etch profile is measured to 76°.

results in a slightly shorter cantilever.

Having showed that the diamond cantilevers can be fabricated with mechanical integrity, and application driven design flexibility, we tested the mechanical robustness of diamond cantilevers. It would be detrimental if cantilevers broke during a measurement, because debris would contaminate valuable samples. Diamond has much higher fracture strength and toughness (Table 1) than silicon, and indeed we observed that the diamond M4PP did not mechanically yield or show any inelastic deformation using our measurement set-up (microRSP-M200, Capres, Denmark). When the diamond cantilevers was pushed into the sample at an 45° incidence angle, it would first deflect and then lay flat on the sample surface. The diamond cantilever only broke if we crashed the silicon support chip into the sample. To push the mechanical conditions to the extreme, we qualitatively tested the yield conditions by applying mechanical forces and observe under which conditions the cantilevers would break. We mounted M4PPs in an SEM with a micromanipulator, and used the manipulator to apply mechanical force to

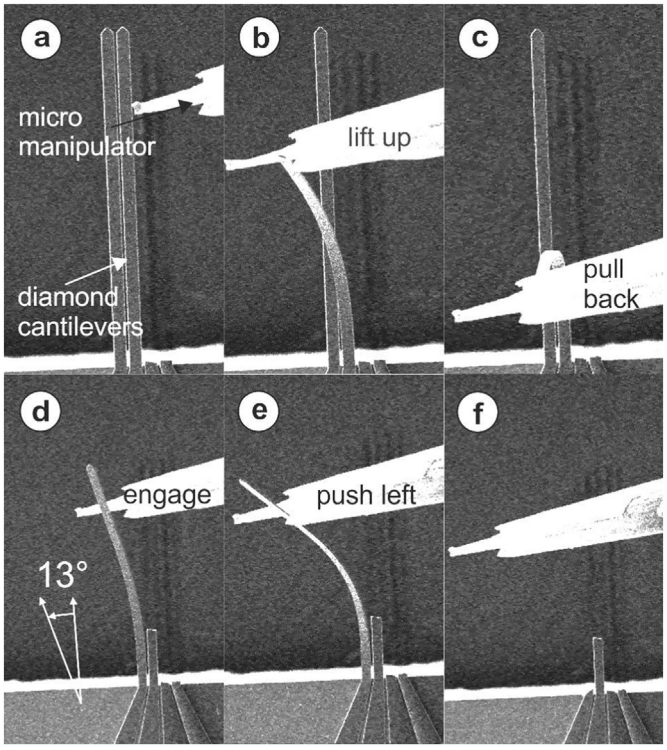

Fig. 5. Micromanipulator is used for testing probe robustness. Probe length is 300 µm. Manipulator engage cantilever from right (a), lifts the cantilever up (b), pull back the cantilever until it breaks (c). Second cantilever is engaged (d), the cantilever is pushed to the left (e) until it breaks (f).

the cantilevers while observing and recording using the SEM. Fig. 5 show six movie frames testing the mechanical robustness of the diamond cantilevers. The diamond cantilevers were 300-µm-long, 8-µm-wide, and 1200-nm-thick. Firstly, we tested how much out-of-plane bending was required to break the cantilever. The cantilevers were

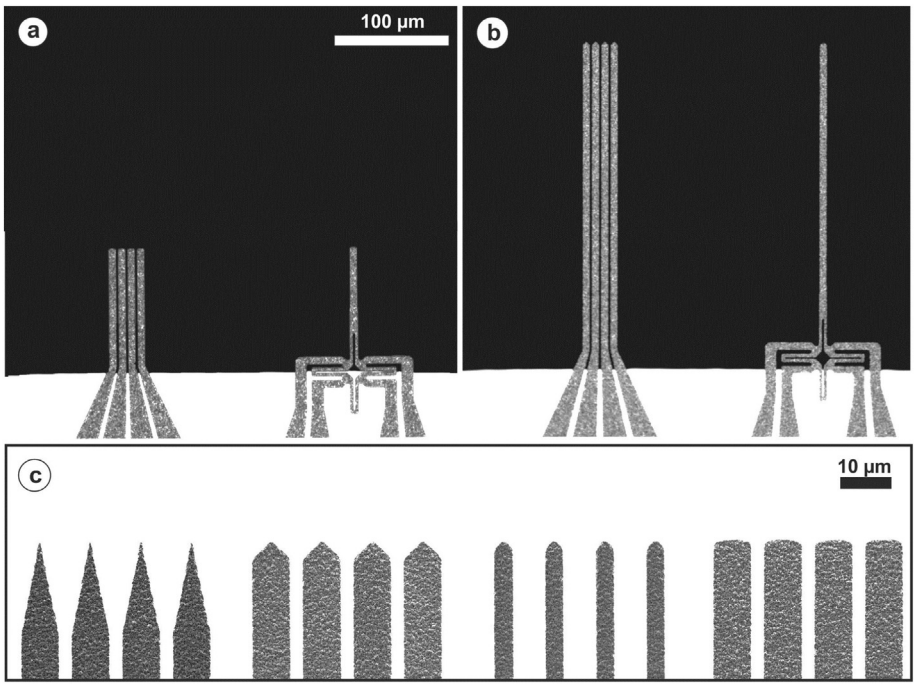

Fig. 4. M4PP for various applications. Optical microscope images of M4PP with integrated strain gauges with cantilever length of respectively 100 µm (a) and 300 µm (b). SEM images of four tip designs (c).

engaged mechanically using the micromanipulator (Fig. 5a). The cantilever is lifted up by 200 µm (Fig. 5b), but this was not sufficient to break it. Then, we pulled the cantilever back by 150 µm, and it folded back forming a bow shape before it broke (Fig. 5c). From the SEM images, and the cantilever geometry, the bending radius at fracture is above 100 µm. The diamond cantilever is 1.2 µm thick, and assuming the neutral axis is in the center of the cantilever, the fracture strain and stress are calculated to respectively < 0.006 and $<$ 5–7 GPa. These values are consistent and slightly higher than previous reports (Table 1). Secondly, we tested how much in-plane bending was needed to break the cantilever. We engaged a second cantilever (Fig. 5d) and pushed to the left (Fig. 5e) until the cantilever broke (Fig. 5f). For angular displacements $< 13^{\circ}$, the cantilever bends to the left without twisting. At larger angular displacements the cantilever twisted because it relaxes to a state with lower mechanical energy. The cantilever breaks at an angular displacement of 33°. For M4PP applications significant inelastic deformation of the cantilevers is not acceptable, because in the most extreme case the cantilevers can touch each other and cause short circuits. Therefore during these tests inside the SEM we looked carefully for inelastic deformation. Even at very large deflections we did not observe inelastic deformation. These robust mechanical properties are more than adequate for diamond cantilevers to be reliably used for the most demanding M4PP applications.

4. Conclusions and outlook

Diamonds superior physical properties motivated us to fabricate polycrystalline diamond M4PP probes. We developed a very straight forward MEMS foundry compatible fabrication process. The process requires only two photolithography masks. The most challenging process step was dry etching of diamond, because there are only few reports and the fact that the etching rates were highly dependent on the etching instruments. We successfully developed a wafer-level process using argon/oxygen ICP plasma and an aluminum etch mask. 330 probes based on 14 different designs were fabricated on a single 100 mm in diameter wafer. Because of the inherent outstanding mechanical properties of diamond, the cantilevers are extremely robust, and we demonstrate that they can be used for the most demanding measurement conditions.

Recently, there has been a tremendous interest in diamond based micro and nanotechnology [6,31]. We believe this will drive the development of more affordable and higher quality diamond substrates in the near future. In this work, we have developed the technology and framework for diamond M4PP, such that when high quality conductive diamond becomes available at a competitive price, we can produce conductive diamond M4PP at MEMS foundries of our choice. Furthermore, we believe that our results will interest the scientific and technology communities working with diamond on the micro and nanoscales [28].

Acknowledgements

The authors would like to thank the Innovation Fund Denmark for financial support. Also, we thank the technical staff at DTU Nanolab. The authors have no competing interests.

Appendix A. Supplementary data

Supplementary data to this article can be found online at https://doi.org/10.1016/j.mne.2019.05.002.

References

[1] J.A. Carlisle, O. Auciello, Ultrananocrystalline diamond, Electrochem. Soc. Interface 12 (1) (2003) 28–31.
[2] M.A. Angadi, et al., Thermal transport and grain boundary conductance in ultrananocrystalline diamond thin films, J. Appl. Phys. 99 (11) (Jun. 2006) 114301.
[3] R.B. Simon, et al., Effect of grain size of polycrystalline diamond on its heat spreading properties, Appl. Phys. Express 9 (6) (2016).
[4] T. Hantschel, P. Niedermann, T. Trenkler, W. Vandervorst, Highly conductive diamond probes for scanning spreading resistance microscopy, Appl. Phys. Lett. 76 (12) (2000) 1603–1605.
[5] J.K. Luo, Y.Q. Fu, H.R. Le, J.A. Williams, S.M. Spearing, W.I. Milne, Diamond and diamond-like carbon MEMS, J. Micromech. Microeng. 17 (7) (2007) S147–S163.
[6] A. Hartl, et al., Protein-modified nanocrystalline diamond thin films for biosensor applications, Nat. Mater. 3 (10) (2004) 736–742.
[7] X.C. Xiao, et al., In vitro and in vivo evaluation of ultrananocrystalline diamond for coating of implantable retinal microchips, J. Biomed. Mater. Res. Part B Appl. Biomater. 77B (2) (2006) 273–281.
[8] L. Sekaric, J.M. Parpia, H.G. Craighead, T. Feygelson, B.H. Houston, J.E. Butler, Nanomechanical resonant structures in nanocrystalline diamond, Appl. Phys. Lett. 81 (23) (2002) 4455–4457.
[9] K. Deng, W.H. Ko, A study of static friction between silicon and silicon compounds, J. Micromech. Microeng. 2 (1) (1992) 14.
[10] X. Li, et al., Measurement for fracture toughness of single crystal silicon film with tensile test, Sensors Actuators A Phys. 119 (1) (2005) 229–235.
[11] H.D. Espinosa, et al., Mechanical properties of ultrananocrystalline diamond thin films relevant to MEMS/NEMS devices, Exp. Mech. 43 (3) (2003) 256–268.
[12] X. Zhao, Y. Liu, Q. Wen, Y. Wang, Frictional performance of silicon carbide under different lubrication conditions, Friction 2 (1) (2014) 58–63.
[13] P. Hess, The mechanical properties of various chemical vapor deposition diamond structures compared to the ideal single crystal, J. Appl. Phys. 111 (5) (2012).
[14] A.R. Konicek, et al., Influence of surface passivation on the friction and wear behavior of ultrananocrystalline diamond and tetrahedral amorphous carbon thin films, Phys. Rev. B - Condens. Matter Mater. Phys. 85 (15) (2012).
[15] S.J. Bull, P.R. Chalker, C. Johnston, V. Moore, The effect of roughness on the friction and wear of diamond thin films, Surf. Coatings Technol. 68–69 (C) (1994) 603–610.
[16] J.D. Buron, et al., Graphene conductance uniformity mapping, Nano Lett. 12 (10) (2012) 5074–5081.
[17] R.J. Hillard, R.G. Mazur, C.W. Ye, M.C. Benjamin, J.O. Borland, A nonpenetrating 4PP measures USJ sheet resistance, Solid State Technol. 47 (8) (2004) 47.
[18] D.H. Petersen, et al., Review of electrical characterization of ultra-shallow junctions with micro four-point probes, J. Vac. Sci. Technol. B 28 (1) (2010) C1C27–C1C33.
[19] F.W. Østerberg, D. Kjær, P.F. Nielsen, O. Hansen, D.H. Petersen, Characterization of magnetic tunnel junction test pads, J. Appl. Phys. 118 (14) (Oct. 2015) 143901.
[20] D.C. Worledge, P.L. Trouilloud, Magnetoresistance measurement of unpatterned magnetic tunnel junction wafers by current-in-plane tunneling, Appl. Phys. Lett. 83 (1) (Jul. 2003) 84–86.
[21] "Capres M4PP."
[22] F. Wang, et al., Three-way flexible cantilever probes for static contact, J. Micromech. Microeng. 21 (8) (Aug. 2011) 85003.
[23] D.H. Petersen, O. Hansen, T.M. Hansen, P.R.E. Petersen, P. Bøggild, Static contact micro four-point probes with $<$ 11nm positioning repeatability, Microelectron. Eng. 85 (5–6) (May 2008) 1092–1095.
[24] I.S. Forbes, J.I.B. Wilson, Diamond and hard carbon films for microelectromechanical systems (MEMS) - a nanotribological study, Thin Solid Films 420 (2002) 508–514.
[25] S.J. Bull, Tribology of carbon coatings - DLC, diamond and beyond, Diam. Relat. Mater. 4 (5–6) (1995) 827–836.
[26] R.A. Oliver, Advances in AFM for the electrical characterization of semiconductors, Rep. Prog. Phys. 71 (7) (2008).
[27] C.L. Petersen, et al., Scanning microscopic four-point conductivity probes, Sensors Actuators A Phys. 96 (1) (2002) 53–58.
[28] S. Castelletto, L. Rosa, J. Blackledge, M.Z. Al Abri, A. Boretti, Advances in diamond nanofabrication for ultrasensitive devices, Microsyst. Nanoeng. 3 (2017) 17061.
[29] D.S. Hwang, T. Saito, N. Fujimori, New etching process for device fabrication using diamond, Diam. Relat. Mater. 13 (11–12) (2004) 2207–2210.
[30] G.F. Ding, H.P. Mao, Y.L. Cai, Y.H. Zhang, X. Yao, X.L. Zhao, Micromachining of CVD diamond by RIE for MEMS applications, Diam. Relat. Mater. 14 (9) (2005) 1543–1548.
[31] I. Aharonovich, S. Castelletto, D.A. Simpson, C.H. Su, A.D. Greentree, S. Prawer, Diamond-based single-photon emitters, Rep. Prog. Phys. 74 (7) (2011).
[32] Y. Ando, Y. Nishibayashi, K. Kobashi, T. Hirao, K. Oura, Smooth and high-rate reactive ion etching of diamond, Diam. Relat. Mater. 11 (3–6) (2002) 824–827.
[33] T. Yamada, H. Yoshikawa, H. Uetsuka, S. Kumaragurubaran, N. Tokuda, S. Shikata, Cycle of two-step etching process using ICP for diamond MEMS applications, Diam. Relat. Mater. 16 (4–7) (2007) 996–999.
[34] B.J.M. Hausmann, et al., Fabrication of diamond nanowires for quantum information processing applications, Diam. Relat. Mater. 19 (5–6) (2010) 621–629.